Investigations of functional and structural changes in migraine with aura by magnetic resonance imaging

Anders Hougaard

This review has been accepted as a thesis together with three previously published papers by University of Copenhagen 22nd of July 2014 and defended on 27th of October 2014.

Tutors: Messoud Ashina, Jes Olesen, Henrik B.W. Larsson, and Sohail M. Asghar.

Official opponents: Cenk Ayata, Jakob Blicher, and Steen Hasselbalch.

Correspondence: Department of Neurology, Rigshospitalet Glostrup, Nordre Ringvej 57, 2600 Glostrup, Denmark

E-mail: ahougaard@dadlnet.dk

Dan Med J 2015;62(8):B5129

THE 3 ORIGINAL PAPERS ARE

1. Hougaard A, Jensen BH, Amin FM, Rostrup E, Hoffmann MB, Ashina M. Cerebral Asymmetry of fMRI-BOLD Responses to Visual Stimulation. PLoS ONE. 2015 May 18.
2. Hougaard A, Amin FM, Hoffmann MB, Rostrup E, Larsson HBW, Asghar MS, et al. Interhemispheric differences of fMRI responses to visual stimuli in patients with side-fixed migraine aura. Hum Brain Mapp. 2014 Jun;35(6):2714–23
3. Hougaard A, Amin FM, Hoffmann MB, Larsson HBW, Magon S, Sprenger T, et al. Structural gray matter abnormalities in migraine relate to headache lateralization, but not aura. Cephalalgia. 2015 Jan;35(1):3–9.

INTRODUCTION

Migraine is a disabling neurological disorder, manifesting primarily as attacks of severe headache accompanied by a wide range of symptoms. It is highly prevalent, affecting approximately 10% of the general population worldwide (4). According to the World Health Organization migraine ranks seventh highest in the world among causes of disability (2). Migraine has substantial socio-economical costs mostly due to absenteeism from work. In the US the economic cost of migraine is estimated at more than USD 23 billion annually (5,6) and in Europe EUR 27 billion annually (7). In order to relieve this global burden of disease better treatment of migraine, and therefore a better understanding of the pathophysiological mechanisms of the disorder, is warranted (8).

MIGRAINE AURA

About one third of migraine patients experience aura, which is defined as gradually developing, transient neurological symptoms, usually occurring before the onset of the migraine headache (9), and most commonly presenting as homonymous visual disturbances (10). Clinically, migraine aura is distinguishable from symptoms of e.g. transient ischaemic attacks and epileptic auras by the characteristic spread of symptoms, usually over 5-20 min for each symptom. Although many variations occur, visual aura typically begins as a vague spot of flickering lights or patterns near the fixation point, which spreads to the lateral part of the field of view. A classic manifestation is the “fortification spectrum”, a definite zigzag pattern, so named because of its resemblance to the fortifications of a castle seen from above. Sensory auras are usually paresthesias, which start in the fingers and spreads towards the upper arm and the head. Both the visual and the sensory symptoms often have a bimodal progression with positive symptoms such as shimmering lights or prickling sensations followed by negative symptoms such as scotoma or numbness. Other aura symptoms include aphasia, hemiparesis and more rare manifestations such as vertigo, tinnitus, diplopia, hearing loss and confusion.

CORTICAL SPREADING DEPRESSION

Based on a clinical evaluation of migraine aura, the character and location of these symptoms clearly point to an origin in the cerebral cortex. In 1941 Lashley, a visual physiologist, published some observations of his own visual auras, including the suggestion that the speed of progression of the visual disturbances corresponded to a wave of excitation propagating over the visual cortical surface at a speed of about 3 mm per minute (11). A few years later, Leão reported his discovery of a spreading decrease of EEG activity following electrical stimulation in the rabbit brain (12). This phenomenon, now known as cortical spreading depression (CSD), was later shown to propagate at a rate of 3 to 5 mm per minute and is now considered to be the underlying cause of migraine aura. CSD is associated with changes in the cerebral blood flow (CBF): a hyperemia phase (more than doubling of flow) followed by a prolonged oligemia phase (i.e. reduced CBF but above the ischemic threshold, lasting more than 1 hour). Changes in CBF characteristic of CSD have been observed migraine patients during aura symptoms in the seminal works by Olesen and Lauritzen (13,14). More recently, a slowly propagating wave of cerebral blood oxygenation level-dependent (BOLD) signal change was recorded during visual aura in a migraine patient using functional magnetic resonance imaging (fMRI)(15). Although direct electrophysiological measurements from the cortical surface has not been performed during migraine aura, slowly propagating depolarizations closely resembling CSD have been observed in unconscious patients following e.g. stroke (16), and head trauma (17). CSD is able to activate trigeminovascular afferents (18) in animals,

and CSD may thus initiate the subsequent headache in migraine patients. Whereas the evidence for CSD underlying migraine aura is firm, it is not known what makes the cerebral cortex of migraine patients with aura susceptible to occasionally exhibiting waves of CSD. Unraveling the CSD-initiating processes may provide important new targets for future migraine treatment.

VISUAL HYPERSENSITIVITY IN MIGRAINE WITH AURA

Many migraine patients with aura report that bright or flickering light can trigger their attacks (19,20), while this is not as often the case for patients without aura (19,21). In mixed populations of patients with and without aura, psychophysical studies have demonstrated increased photosensitivity (22,23) and aversion to the exposure to certain visual patterns (24) outside of attacks. Transcranial magnetic stimulation (TMS) studies, although conflicting, generally found lower thresholds for the induction of visual perception (phospenes) in migraine with aura compared to controls (25), suggesting visual cortical hyperexcitability. Based on these observations it has been suggested that an increased responsiveness, especially to visual stimuli, in the interictal state predisposes migraine patients to developing attacks, possibly by triggering CSD (reviewed in (26,27). Accordingly, in rabbits CSD can be elicited by directing light flashes into the animal's eyes, following intravenous administration of pentylenetetrazol, a GABA-A receptor blocker (28).

FUNCTIONAL MAGNETIC RESONANCE IMAGING

Functional magnetic resonance imaging (fMRI) is a neuroimaging technique for measuring brain activity by detecting associated changes in CBF. The most commonly used form of fMRI is based on the blood oxygenation level dependent (BOLD) signal, which relies on the different magnetic properties of oxygenated and deoxygenated hemoglobin. Cerebral neuronal activity causes the regional CBF to increase (neurovascular coupling). As a consequence more oxygenated blood is delivered to the active area than is needed by the active neurons. This local increase in oxygenated blood implies that the local concentration of deoxyhemoglobin decreases. Deoxyhemoglobin distorts the magnetic field and thereby attenuates the MRI signal. The BOLD signal reflects MRI signal changes caused by field inhomogeneity, and therefore an increase of neuronal activity can be detected as an increase of the BOLD signal in an MR scanner. The measured activation using this method most likely reflects the input and local processing of neuronal information within a region, rather than the neuronal output (29). Due to its relatively high spatial resolution fMRI has the potential not only to detect, but also to localize hypersensitive cortex. There are only few fMRI studies of cortical responses to visual stimulation during the interictal state of migraine with aura and results are inconsistent (30-32).

INTERHEMISPHERIC COMPARISON

Aura symptoms are mostly half-sided (10), indicating involvement of one cerebral hemisphere. From an investigational viewpoint this advantageously offers the possibility of studying the disease by using the unaffected hemisphere as control. In such a comparison, variation due to physiological processes during the investigation, such as heart and respiratory rates, hormonal and electrolyte levels, as well as sources of variation from the investigational procedure, e.g. measurement noise, are all cancelled out. This low variability makes the side-to-side comparison design more sensitive and accurate than a longitudinal design in which a subject is examined at two different time points and much superior to a comparison of independent groups, e.g. patients compared to healthy controls.

To investigate the features of migraine aura, an ideal approach would therefore be to compare affected cerebral hemispheres to the contralateral, non-affected hemispheres of the same patients. A challenge to this approach is the fact that the affected side often changes from attack to attack and the symptoms rarely occur consistently on the same side (10). Some patients, however, experience aura symptoms on the same side in every attack. The interhemispheric comparison approach has previously been applied to MRI data for comparison of grey matter structure (33,34) and for assessment of hemispheric language dominance (35) but not for interhemispheric comparison of cortical responses to visual stimulation.

SPECIFIC AIMS

- To validate a method for comparing fMRI data of responses to visual stimulation between the two cerebral hemispheres and apply this method to compare visual activation between left and right hemispheres in healthy subjects
- To investigate if migraine with side-fixed visual aura is associated with functional changes in the visual system, as assessed by BOLD-fMRI
- To investigate if migraine with side-fixed visual aura is associated with structural cortical changes, as assessed by MRI-based morphometry

METHODS

PARTICIPANTS

We recruited 60 healthy controls (36 F, 24 M, mean age 35.4 years [range 19 - 61]). We also included 20 patients (15 F, 5 M, mean age 35.0 [range 20.7 – 55.0]) suffering from migraine with typical aura (MA) according to the second edition of The International Classification of Headache Disorders (36). Inclusion criteria for the patients were unilateral, homonymous visual aura occurring on the same side (either the left or the right hemifield) in 90% of attacks or more and an attack frequency of 1 attack per month or more. An equal number of patients with right- and left-sided symptoms were included, i.e. 10 patients with symptoms in the right visual field, and 10 with symptoms in the left visual field. Twenty of the healthy controls were individually age and sex matched to the migraine patients (15 F, 5 M, mean age 35.1 [range 20.6 – 54.7]). Exclusion criteria for both groups were: Any type of non-migraine headache (except for tension-type headache 3 days per month or less); serious somatic or psychiatric conditions; intake of daily medication including prophylactic migraine treatment; ineligibility of being MR scanned (e.g. metal implants, pregnancy, and claustrophobia). We excluded healthy controls with a history of any type of migraine or first-degree relatives with a history of any type of migraine. Patients and controls had a general medical history taken and underwent a neurological examination. All participants reported normal or corrected to normal vision. In addition, we assessed handedness, visual acuity and ocular dominance in healthy controls. Handedness was assessed using the Edinburgh Handedness Inventory(37). Decimal visual acuity was determined with the Freiburg Acuity and Contrast Test (FrACT)(38), i.e. Landolt-C optotypes displayed on an LED display (22 inch Brilliance 220SW LED display, 1680 x 1050 pixels; Philips, Best, The Netherlands) at a viewing distance was 3 meters. Eye dominance was examined using the 'hole in hand' variant of the Miles test (39).

GENERAL STUDY INFORMATION

Patients and controls reported headache-free to the research facility on the study day, i.e. all patients were studied in the interictal phase. Following interviews and examination all participants underwent functional and structural MRI (see below). The studies were carried out at Glostrup Hospital, Copenhagen, Denmark from April 2011 to July 2013. All subjects gave informed consent to participate in the studies. The studies were approved by The Ethics Committee of the Capital Region of Denmark.

MRI PROCEDURE (STUDIES I-III)

MRI was performed on a 3.0T Philips Intera Achieva scanner (Philips Medical Systems, Best, The Netherlands) using a 32-element phased-array receive head coil. Anatomical images were acquired using a T1-weighted three-dimensional turbo field-echo sequence (170 sagittal slices of 1 mm thickness; in-plane resolution 1 x 1 mm; repetition time 9.9 s; echo time 4.6 ms; and flip angle 81 deg).

Functional imaging used a gradient-echo echo-planar imaging sequence (32 slices of 4.0 mm thickness; slice gap 0.1 mm; field of view 230 x 230 mm; in-plane acquired resolution 2.9 x 2.9 mm; repetition time 3.0 s; echo time 35 ms; flip angle 90 degrees; and SENSE (SENSitivity Encoding) factor 2). Phase encoding was carried out in the anterior-posterior direction to avoid left-right asymmetry. Dummy scans (two volumes) were applied to ensure steady-state longitudinal magnetization. Heart rate and respiratory frequency was monitored during the scanning procedure. The lighting conditions inside the scanner and in the scanner room were identical in each scan session.

Visual stimulation was presented using OLED video goggles (NordicNeuroLab, Bergen, Norway; SVGA, 800 x 600 pixels, refresh rate 85 Hz, FOV 30° horizontal, 23° vertical, stimulus luminance: 70-110 cd/m2). A fiber optic cable connected the system to a control computer outside the scanner room. The block-design stimulation paradigm consisted of an alternation of stimulation and rest blocks each comprising 18 s. During stimulation blocks a symmetrical full-field high contrast motion stimulus was presented i.e., a moving black and white dartboard pattern [diameter: 22 deg (circular aperture); ring width: 0.6 deg; spoke width: 15 deg; patterns in each spoke moved in opposite directions, alternately inward and outward, with random changes of the motion direction approx. every 2-3 s]. The stimulus was generated using freely available Matlab-based software (http://vistalab.stanford.edu/software). A complete scan comprised thirty-two 18 s blocks and lasted 576 s. The subjects were instructed to fixate on a central fixation point during the entire scan. They performed no additional stimulus driven task (e.g. button press) to avoid task related effects on response lateralization(40). The onset of visual stimulation was triggered by the scan acquisition.

VALIDATION EXPERIMENT (STUDY I)

To validate the method of functional interhemispheric comparison, we initially conducted an experiment in which healthy subjects were stimulated in one visual hemifield at a time, to compare “activated” hemispheres (contralateral to the stimulation) to the opposite “non-activated” hemispheres (Fig. 1). This experiment was conducted to assess the effects of data flipping, averaging and registration to a symmetrical standard space (see below). Five of the included healthy volunteers participated in this experiment (1 F, 4 M, mean age 29.6 years [range 24.3 - 37.2 years]). Each subject was scanned twice using the procedure and visual stimulation described above, but with unilateral stimulation: one scan with stimulation in the left hemifield and one scan with stimulation in the right hemifield.

Figure 1:

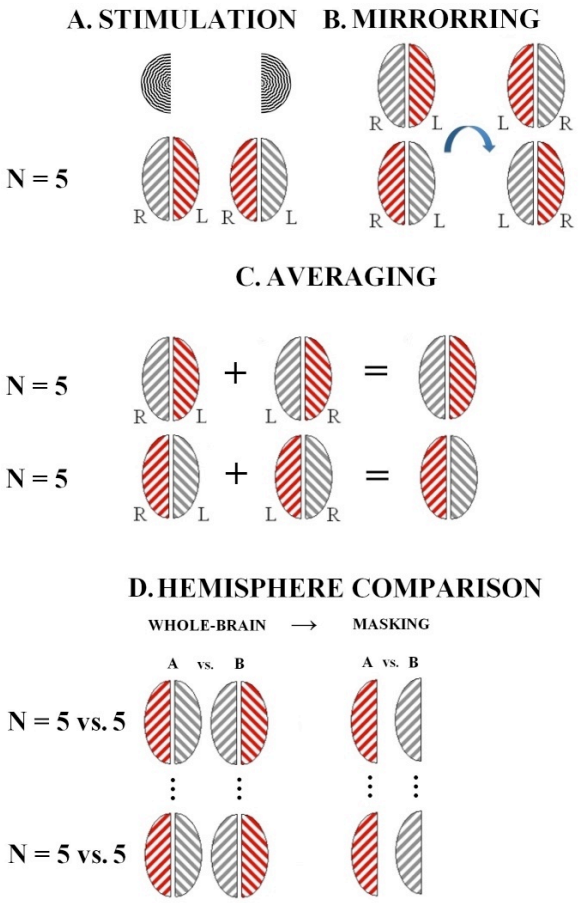

(a) Two scan sessions were carried out in five subjects out during visual stimulation of the left and right hemifield, respectively. (b) Left-right mirrored copies of the acquired data were created for each scan session. (c) After processing the first-level fMRI results, left hemifield stimulation images were averaged with mirrored right hemifield images and vice versa. Thus, ”activated” hemispheres, contralateral to the stimulation, are averaged in the same side of the image space. (d) Hemispheres were compared in a higher-level analysis. A paired analysis of brains with the ”activated” hemispheres in the right side of image space vs. corresponding mirrored images was carried out. This would produce the same results (with opposite sign) for both hemispheres. To avoid this redundancy the left side of the image space was zeroed by a binary mask, thus performing calculations on the right side only.

GOGGLE POSITION (STUDY I)

Fifty-six healthy volunteers, including one subject from the validation study, were stimulated using the full-field stimulation as described above. These subjects underwent one scan with the video goggles in the standard position and one scan with the goggles rotated 180 degrees to control for lateralization effects caused by asymmetry of the stimulation (Fig. 2). The sequence of goggle positions was changed every time a new subject was scanned to avoid differences between scans obtained in the two positions to be due to time effects.

DATA ANALYSIS (STUDIES I-III)

The main objective of the analysis was to compare functional activation in response to visual stimulation between cerebral hemispheres: “stimulated” vs. “non-stimulated” hemispheres for the validation experiment (Study I), left vs. right hemispheres for

the study of healthy subjects (Study I) and symptomatic vs. asymptomatic hemispheres for the migraine aura patients (Study II). In addition grey matter structure was compared between symptomatic and asymptomatic hemispheres (Study III). This was primarily achieved by direct comparison of voxels in hemispheres to corresponding voxels in the contralateral hemispheres by comparing image data in the standard radiological convention to mirrored data (i.e. flipped horizontally in the left-right direction, see Fig. 3). Hemispheres were also compared using a region of interest (ROI) based approach and, for structural data, a vertex-wise comparison (see "Surface-based morphometry").

Figure 2:

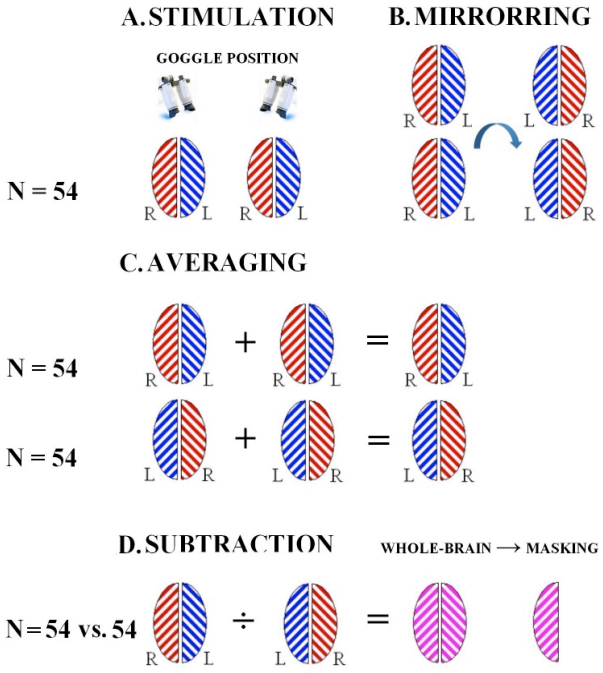

(a) Two scan sessions were carried out in 54 subjects out during full-field visual stimulation: one with the stimulation goggles in the standard position and one with the goggles flipped 180 degrees. (b) Left-right mirrored copies of the acquired data were created for each scan session. (c) After processing the first-level fMRI results, data from the two scan sessions were averaged for each subject. (d) First-level results of mirrored data were subtracted from first-level results of data in the original orientation to produce left-right difference images that would allow for adding covariates to the model. The difference images have the same values in the right and left sides of image space but with opposite signs. To avoid this redundancy the left side of the image space was zeroed by a binary mask.

FUNCTIONAL MRI ANALYSIS (STUDIES I-II)

Analysis of the fMRI images to identify regions exhibiting significant stimulus-correlated changes in blood oxygen level dependent (BOLD) signal was carried out in a multi-stage process using FMRIB's Software Library (FSL) ver. 4.1.19(41).

IMAGE PRE-PROCESSING AND ALIGNMENT

Mirror images of the acquired functional and anatomical data were created for each subject. In order to avoid left-right bias from registration to an asymmetrical standard space, a symmetrical version of the Montreal Neurological Institute (MNI) 152 template was created by adding a mirrored version of the template to the original version (35). The T1-weighted high-resolution anatomical scans were brain-extracted (i.e. non-brain structures were removed) using FSL BET. Functional data were registered (aligned) to the brain extracted images and to the symmetrical MNI152 template using FSL FLIRT linear registration. Registration from high resolution structural to standard space was further refined using FSL FNIRT nonlinear registration. Mirrored functional images were registered to the corresponding mirrored T1-weighted images.

FIRST-LEVEL VOXEL-WISE ANALYSIS

First-level analysis of the functional data was carried out using FSL FEAT (FMRI EXPERT Analysis Tool) ver. 5.98. Pre-processing included slice time correction, spatial smoothing (FWHM 5 mm), high pass filtering (cut-off 36 s), head motion correction using FSL MCFLIRT and brain extraction of functional and anatomical images using FSL BET. After pre-processing, a voxel-based analysis was performed using a general linear modeling approach, with local autocorrelation correction, of seven regressors (main stimulus (box-car), a temporal derivative and six motion regressors) convolved with a canonical single gamma hemodynamic response function. Z (Gaussianized T) statistic images were thresholded using clusters determined by $Z > 2.3$ and a corrected cluster significance threshold of $P < 0.05$ (using a distribution based on Gaussian Random Field Theory). Mean activation and deactivation maps of all scan sessions from eligible subjects was calculated using a fixed-effects analysis in FSL-FEAT.

VALIDATION EXPERIMENT (STUDY I)

After processing the first-level fMRI results, left-hemifield stimulation images were averaged with mirrored right-hemifield stimulation images and vice versa using a fixed-effects analysis in FSL-FEAT (Fig. 1c). Thus, "activated" hemispheres, contralateral to the stimulation, were averaged in the same side of the image space. A paired analysis of brains with the "activated" hemispheres in the right side of image space vs. corresponding mirrored images was carried out using FSL-FLAME. The null-hypothesis was no average difference between "activated hemisphere" and "non-activated hemisphere". As in the first-level analysis, Z statistic images were thresholded using clusters determined by $Z > 2.3$ and a corrected cluster significance threshold of $P < 0.05$ (using a distribution based on Gaussian Random Field Theory). This analysis would produce the same results (with opposite sign) for both hemispheres. To avoid this redundancy the left side of the image space was zeroed by a binary mask. For the method to be considered valid this should show activation differences in relevant brain areas for the contrast "activated hemisphere" > "non-activated hemisphere" and no differences for "non-activated hemispheres" > "activated hemispheres". The results of this analysis are shown in Fig. 4.

GOGGLE POSITION (STUDY I)

We assessed if the goggle position per se would cause differences in the activation pattern following full-field visual stimulation. A second-level paired voxel-wise group comparison was carried out using FSL FLAME (goggles in the standard position vs. goggles rotated 180 degrees). We found no differences in activation between the two goggle positions.

Comparison of left vs. right hemispheres (Study I)

To compare left and right hemispheres of the healthy subjects, data in the original orientation were compared to mirrored data (Fig. 2b). Functional data from the two goggle positions were averaged for each subject (Fig. 2c). Followingly, left-right difference maps were calculated by subtracting first-level results of mirrored data from first-level results of original data in a fixed-effects analysis (Fig. 2d). To investigate the sources of interhemispheric

differences, we analyzed left-right difference maps from each subject in a general linear model with six subject-dependent regressors: mean effect, handedness, interocular difference in visual acuity, age, gender, and one voxel-dependent regressor (anatomical grey matter probability maps created using the FSL script feat_gm_prepare (42)). The latter integrates a voxel-based morphometry grey matter map (difference between right and left hemisphere) into the analysis to correct for functional activation differences due to differences in grey matter volume. The analysis was performed using FSL-FLAME. As in the first-level analysis, Z statistic images were thresholded using clusters determined by Z > 2.3 and a corrected cluster significance threshold of P < 0.05.

COMPARISON OF SYMPTOMATIC VS. ASYMPTOMATIC HEMISPHERES (STUDY II)

Functional activation of the symptomatic hemispheres (i.e. contralateral to the visual symptoms) of the patients was compared to the activation level of their contralateral asymptomatic hemispheres (Fig. 1). Since right-sided and left-sided symptoms were reported by an equal number of patients, an equal number of right and left symptomatic hemispheres were analyzed. Thus, any differences between right and left hemispheres (e.g. caused by physiological left/right bias, asymmetry of the visual stimulation or magnetic field inhomogeneity of the scanner) would be expected to cancel each other out in the analysis. Study I showed that left-right functional asymmetry of the healthy brain also depends on age. Patients with left-sided and right-sided symptoms were of equal age (mean age 34.7 years for left-sided vs. 35.2 years for right-sided). The symptomatic hemispheres were also compared to the corresponding hemispheres in age and sex-matched healthy controls, as were the asymptomatic hemispheres (e.g. for a patient with left-sided symptoms, the symptomatic right hemisphere was compared to a right hemisphere in a healthy control of same age and sex).

Initially, hemispheric comparison was carried out using a voxel-wise approach following the same method as in the validation experiment (Fig. 1).

Subsequently, hemispheres were compared using a ROI-based approach. Values from ROIs were extracted from the previously calculated FSL-FEAT results using featquery (a part of the FSL software package). ROIs were mask images derived from the results of the voxel-wise analyses, from Freesurfer segmentations (see below) or ROIs from the Jülich histological (cyto- and myeloarchitectonic) atlas (43). The values used for calculations were the median percentual signal changes during activation.

For ROIs derived from the voxel-wise analysis values were extracted from functional data registered to the symmetrical version of the MNI-template. For all other ROIs, values were extracted from functional data registered to the standard MNI152 2mm template. Statistical calculations were carried out using R ver. 2.14.1 for MacOS X. Values of ROIs were compared using paired T-tests corrected for multiple comparison using the sequential Bonferroni correction after Holm (44).

Individual visual area ROIs were created for each subject by cortical reconstruction and volumetric segmentation of the acquired high-resolution T1-weighted images using the FreeSurfer image analysis suite (http://surfer.nmr.mgh.harvard.edu/)(45,46). In this procedure spatial probability maps of different Brodmann areas were created. An accurate prediction of primary visual cortex (V1) based on cortical folds (47) was furthermore carried out. The latter method has a very high agreement with fMRI retinotopic mapping for the identification of V1 (48). In Freesurfer only the following visual area definitions are provided: Primary visual cortex (V1), secondary visual cortex (V2) and visual area V5/MT. To expand the analysis to other areas, we additionally evaluated ROIs provided by the Jülich atlas (43) i.e. visual areas V3 and V4 and the lateral geniculate nucleus (LGN).

Figure 3:

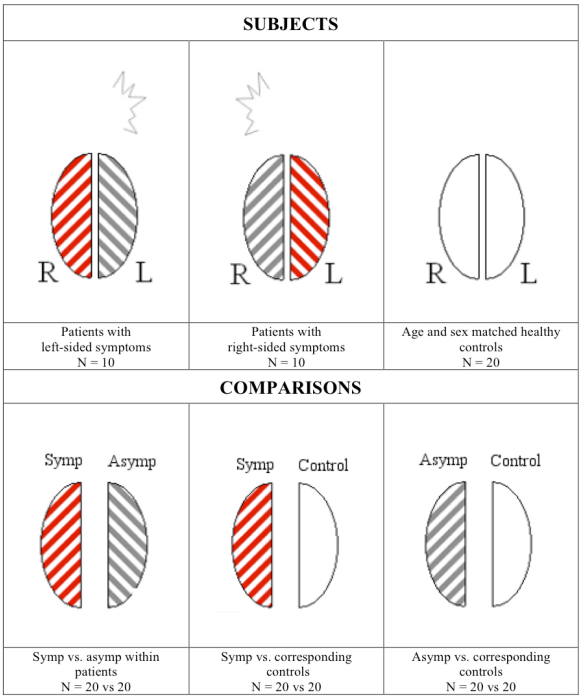

Hemispheres of patients with visual aura symptoms consistently originating from either the right (N=10) or the left (N=10) hemisphere are examined. Symptomatic (Symp) hemispheres (red stripes) of the patients (N=20) are compared to their contralateral asymptomatic (Asymp) hemispheres (grey stripes, N=20). Subsequently, the symptomatic and asymptomatic patient hemispheres are compared to hemispheres of matched healthy control subjects (white). Left patient hemispheres are compared to left control hemispheres and vice versa.

STRUCTURAL MRI ANALYSIS (STUDY III)

Grey matter structure was compared between the symptomatic and asymptomatic hemispheres of the patients using two different techniques: voxel-based morphometry (VBM) and surface-based morphometry (SBM). While cortical thickness is selectively measured using the SBM-based method, VBM provides a mixed measure of grey matter including cortical density, as well as cortical thickness (49). Thus, a combination of these two complimentary methods is useful to both detect and specify the underlying grey matter changes. As a secondary endpoint, we compared interhemispheric differences with regard to headache side.

VOXEL-BASED MORPHOMETRY

Structural data were analyzed with FSL-VBM (http://fsl.fmrib.ox.ac.uk/fsl/fslwiki/FSLVBM)(50), an optimized VBM protocol (51) carried out with FSL tools (52). Before the analysis, mirror images of the acquired anatomical data were created for each subject by flipping the images along the x-axis. The brain was extracted using the structural images and grey matter segmentation was performed before the images were registered to the Montreal Neurological Institute (MNI) 152 standard space using non-linear registration (53). The resulting images, mirrored and original data, were averaged to create a left-right symmetric, study-specific grey matter template. Second, all native grey matter images were non-linearly registered to this

study-specific template and "modulated" to correct for local expansion (or contraction) due to the non-linear component of the spatial transformation. The modulated grey matter images were then smoothed with an isotropic Gaussian kernel with a sigma of 3 mm, i.e. approximately full width half maximum (FWHM) of 3x2.3 = 6.9 mm. Finally, images in the original orientation were compared to the corresponding mirrored images in a paired fashion by application of voxel-wise general linear model (GLM) using permutation-based non-parametric testing (54), correcting for multiple comparisons across space by threshold-free cluster enhancement (55) (cluster-wise P < 0.05).

SURFACE-BASED MORPHOMETRY

Cortical reconstruction and volumetric segmentation was performed with the FreeSurfer image analysis suite (45,46). Using this approach, the grey and white matter surfaces were defined by an automated brain segmentation process. An experienced investigator, who was blinded with respect to the symptomatic hemispheres of the subjects, then manually corrected the automated segmentation. Cortical thickness was estimated at each point across the cortex by calculating the distance between the grey/white matter boundary and the cortical surface. Individual whole brain (right and left hemisphere) surface maps were then registered to a common FreeSurfer template surface pseudo-hemisphere (fsaverage_sym)(56) by the FreeSurfer spherical registration system(57) and smoothed with a 10 mm 2D Gaussian smoothing kernel(57). Symptomatic and asymptomatic hemispheres were statistically compared in a paired design while applying cluster-wise correction for multiple comparisons using a permutation-based non-parametric analysis (cluster-wise P < 0.05). Additionally, we measured the volume of the thalamus, caudate, putamen, amygdala and hippocampus bilaterally for each subject using FreeSurfer's automated subcortical segmentation.

Region of interest analysis

Several ROIs were examined for focal changes of grey matter using both VBM and SBM. We investigated the following ROIs parcellated by FreeSurfer: Primary visual cortex (V1), secondary visual cortex (V2), visual area V5/MT and somatosensory cortex (SSC, Brodmann areas BA1, BA2, BA3a and BA3b). Furthermore, we examined the following ROIs, which are not available in FreeSurfer, using the FSL version of the Jülich histological atlas (43): Visual area V3, visual area V4 and the lateral geniculate nucleus (LGN).

Finally, we specifically checked, whether the hyperresponsivity of the symptomatic hemispheres with respect to aura, observed in study II (see Results), is directly related to changes of cortical morphology. This was done for all ROIs for which hyperresponsivity was observed (inferior frontal gyrus, superior parietal lobule and inferior parietal parietal lobule) by correlating the BOLD to visual stimulation to the mean cortical density (VBM results) and mean cortical thickness (SBM results) of these areas. Statistical calculations were carried out using R ver. 2.14.1 for MacOS X. Mean cortical thickness and mean grey matter density for each ROI was compared using paired T-tests corrected for multiple comparison using the sequential Bonferroni correction according to Holm (44).

RESULTS

All subjects completed the study. One healthy subject was excluded because she fell asleep during one of the two functional scans. All other subjects complied well with the study procedures. The T1-weighted images were reviewed by an experienced neuroradiologist who found a structural abnormality in one healthy subject, causing this subject to be excluded. The neuroradiologist reported no structural abnormalities in the patients.

FUNCTIONAL MRI ANALYSIS (STUDIES I-II)

Validation experiment (Study I)

Comparing "activated" to "non-activated" hemispheres in five subjects showed a marked activation in the occipital lobe, peaking in the primary visual cortex (MNI coordinates (x, y, z) = (-14, -94, 8)) for "activated" > "non-activated" hemispheres and no difference for "non-activated" > "activated" hemispheres. See Fig. 4.

Figure 4:

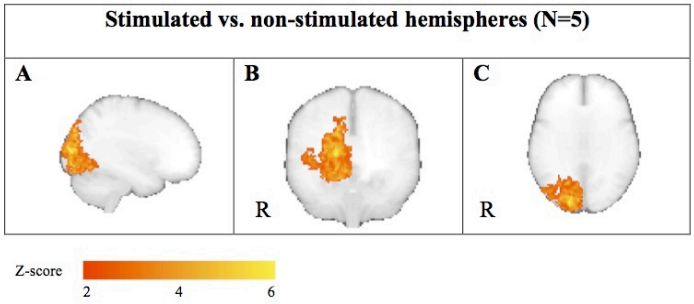

Maximum intensity projections ("glass-brain") presentations of the voxel-wise results from the interhemispheric comparison analyses. Right>Left activation is shown on the right side while Left>Right activation is shown on the left side.

Average activation (Study I)

We found no differences between stimulation with the goggles placed in the standard position compared to scans performed with the goggles rotated 180 degrees. Thus, the goggle position did not cause any asymmetry of cortical activation. Averaging all 108 scans from the 54 eligible healthy subjects showed that the stimulation was able to activate a large part of the cerebral cortex (Fig. 5).

Figure 5:

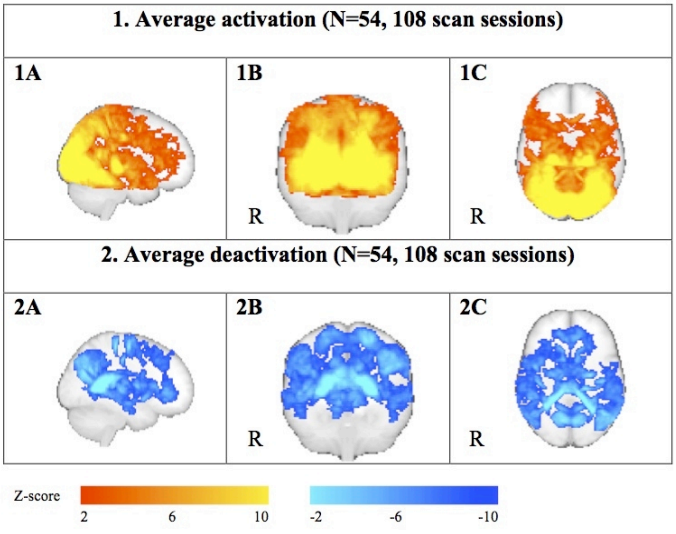

Maximum intensity projections of the average activation and deactivation for all scan sessions (2 sessions with 2 different goggle positions in all eligible subjects). Due to the high power of the approach great expanses are activated, which creates the impression that activation and deactivation appear to overlap locally. Both maps are, however, exclusive.

Comparison of left vs. right hemispheres (Study I)

In the healthy subjects the voxel-wise interhemispheric comparison showed a lateralized activation in response to the symmetrical visual stimulation. Most asymmetrically activated areas were lateralized to the right hemisphere (Fig. 6). This asymmetry of visual cortical activation was partly explained by a larger grey matter density of the right visual cortex (Fig. 6C) and it was age-dependent for one area in the parietal cortex (less right-ward lateralization with increasing age, Fig. 6B). The asymmetry was not related to handedness, interocular difference in visual acuity or ocular dominance.

Figure 6:

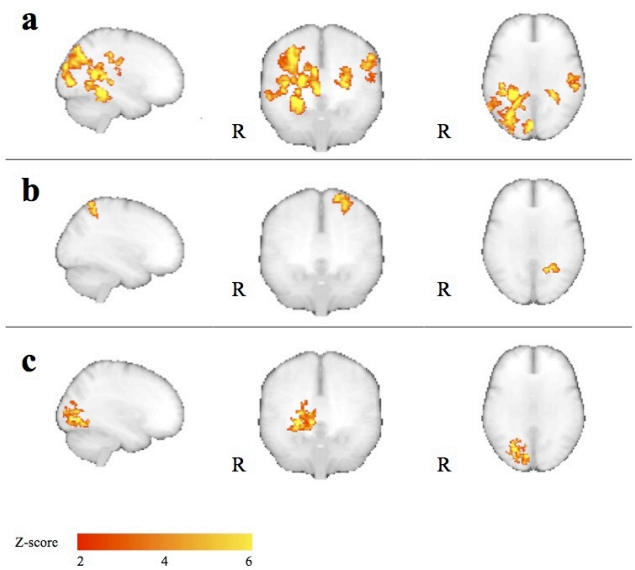

Maximum intensity projections ("glass-brain") presentations of the voxel-wise results from the interhemispheric comparison analyses. Right>Left activation is shown on the right hemisphere side (marked "R") while Left>Right activation is shown on the left side. (a) Left-to-right activation differences corrected for six different parameters (See text). (b) and (c) Differences that correlate positively with age and grey matter volume, respectively.

Comparison of symptomatic vs. asymptomatic hemispheres (Study II)

The voxel-wise analysis revealed multiple areas of significantly higher activation levels in the symptomatic compared to the contralateral asymptomatic hemispheres. Significantly lower activation was not detected anywhere in the symptomatic hemispheres. Fig. 7A shows "glass brain" maximum intensity projections of these voxel-wise results. The most significant voxel clusters were in the inferior frontal gyrus (561 voxels, most significant voxel MNI coordinates (x,y,z) = (-38,36,16), P= 8.5 .10-6), in the superior parietal lobule (SPL)/intra-parietal sulcus (IPS) (324 voxels, (-18,-62,50), P=0.0013), in the inferior parietal lobule (IPL) (234 voxels, (-60, -40, 38), P=0.011) and in a separate cluster of the inferior frontal gyrus, possibly corresponding to the pars opercularis (195 voxels, (-46, 10, 16), P=0.03). A detailed account of the individual results for these areas is given in Fig. 8. In this quantitative ROI analysis the largest signal increases in the symptomatic hemisphere were evident for the cluster superior parietal lobule/intra-parietal sulcus. In the asymptomatic hemisphere median percentual signal changes are negative for some of the clusters analyzed. This signal decrease is most pronounced for the cluster inferior parietal lobule/supramarginal gyrus. No significant differences were found for the occipital lobe or LGN ROIs. Comparison of mean instead of median percentual signal changes provided the same statistical conclusions for the paired T-test and the sign test.

We did not find correlations between the level and direction of asymmetry and the attack frequency or disease duration.

In the voxel-wise comparison of symptomatic hemispheres in patients to corresponding hemispheres in controls (Fig. 7B), we found an activation pattern similar to that of the within-patient analysis, and no differences when comparing asymptomatic hemispheres to corresponding controls (Fig. 7C). No voxels had significantly higher activity in hemispheres of controls than in hemispheres of patients. Accordingly, the individual results indicate significantly higher activations in symptomatic than in corresponding control hemispheres for all four clusters identified above, but no differences between asymptomatic patient hemispheres and controls in any clusters (Fig. 8). No significant differences were found for the occipital lobe or LGN ROIs. No statistical voxel-wise differences were found in a whole-brain comparison of patients versus controls with images from both groups in the original orientation.

Figure 7:

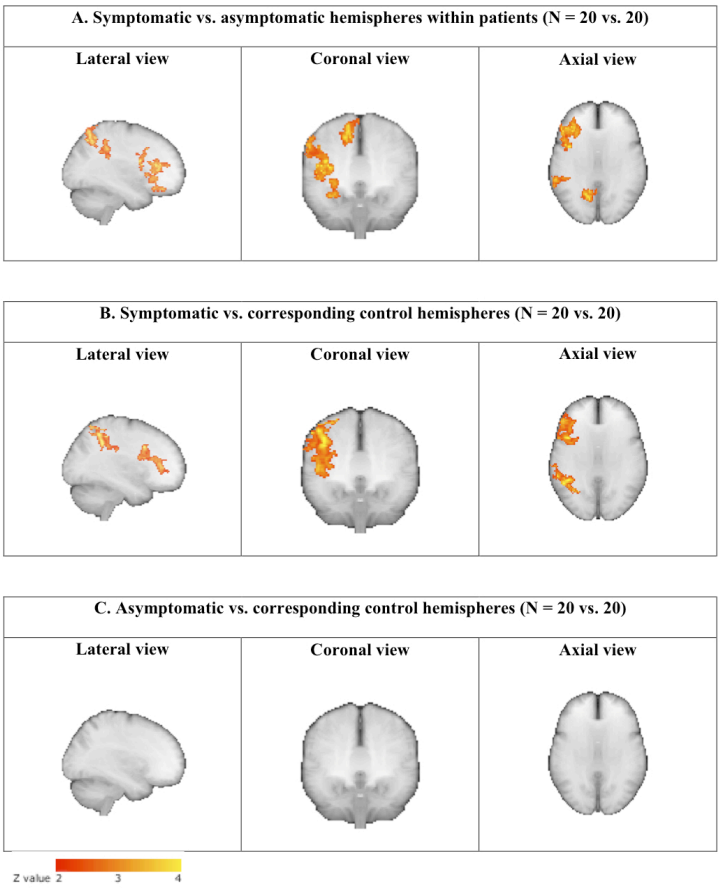

Maximum Intensity Projections ("Glass brain") from the voxel-wise hemisphere comparisons of the fMRI-BOLD responses to visual stimulation. The significantly activated three-dimensional areas are projected onto different two-dimensional planes: lateral, coronal and axial. Symptomatic hemispheres of the patients are compared to their contralateral asymptomatic hemispheres (A). Then the symptomatic and asymptomatic patient hemispheres are compared to hemispheres of matched healthy controls (B and C).

Figure 8:

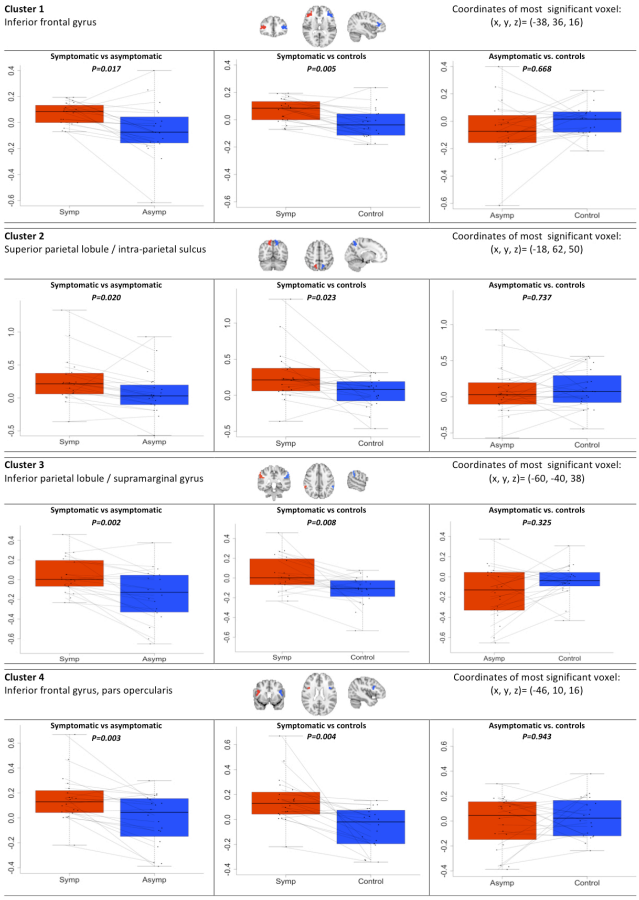

ROI-based results from extracted clusters. The fMRI-BOLD activation levels in the four significant clusters of activation from the voxel-wise comparison of symptomatic and asymptomatic patient hemispheres. For each cluster a comparison of symptomatic hemispheres (symp) to the contralateral asymptomatic hemispheres (asymp) within patients is shown. Also shown are comparisons of the symptomatic and asymptomatic patient hemispheres to hemispheres of matched healthy control subjects. Activation levels were compared using paired T-tests corrected for multiple comparison using the sequential Bonferroni correction after Holm. Values on y-axes are median percentual BOLD signal changes during activation.

STRUCTURAL MRI ANALYSIS (STUDY III)

Voxel-based morphometry

Voxel-wise whole-hemispheric comparison of symptomatic versus asymptomatic hemispheres with regard to aura showed no differences. We found no differences of regional grey matter density in any of the examined ROIs. There was no correlation between the functional activation of hyperresponsive ROIs (Study II) and the mean VBM grey matter density values. Comparing the typical headache side to the non-headache side did not reveal any side-to-side differences for the voxel-wise whole-hemisphere comparison or the ROI based analysis, either.

Surface-based morphometry

We found no differences for the whole-hemisphere or ROI based comparison of symptomatic and asymptomatic hemispheres with regard to aura. There was no correlation between the functional activation of hyperresponsive ROIs (Study II) and the cortical thickness of these ROIs.

For the comparison of headache side versus non-headache side (patients with unilateral headache, N=13), the whole-hemispheric analysis showed a between-hemisphere difference corresponding to an increased cortical thickness in the hemispheres contralateral to the perceived headache side in the pars opercularis of the inferior frontal gyrus (mean between-hemisphere difference 0.12 mm, SD 0.64 mm, cluster-wise P = 0.036, MNI coordinates x, y, z = -46, 17, 21), see Fig. 9. No differences were seen for the a priori specified ROIs or for volumes of subcortical structures. A subsidiary analysis comparing left and right hemispheres revealed no differences in frontal cortical thickness. Further, no interhemispheric differences in the volume of thalamus, caudate, putamen, amygdala or hippocampus were found between symptomatic and asymptomatic or between headache and non-headache side.

An additional, exploratory analysis showed a correlation between the difference in cortical thickness of the pars opercularis ROI between the pain and non-pain sides in patients with unilateral headache and the attack frequency (n=13, Pearson's product-moment correlation, P = 0.005). We did not find a correlation between the mean (left and right) cortical thickness of this ROI and the attack frequency (N=20, Pearson's product-moment correlation, P = 0.32).

Further, comparing the mean cortical thickness of the ROI between patients with unilateral versus patients with bilateral headaches did not show any difference (N= 13 vs. 7, Two-sample t-test, P = 0.87). Additional whole-brain comparisons of patients with unilateral versus bilateral headache (VBM and SBM) also did not reveal any structural differences.

Figure 9:

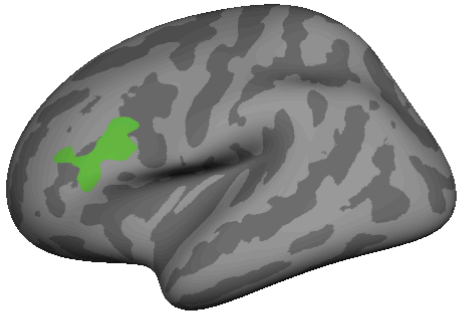

Results of interhemispheric comparison of headache side (N=13) versus non-headache side (N=13). A statistically significant cluster of difference in cortical thickness (non-headache side minus headache side) was found exclusively in the pars opercularis of the inferior frontal gyrus (mean between-hemisphere difference 0.12 mm, SD 0.64 mm, cluster-wise P = 0.036, MNI coordinates x, y, z = -46, 17, 21).

DISCUSSION

INTERHEMISPHERIC COMPARISON AND CEREBRAL ASYMMETRY (STUDY I)

Study I provided very useful information for the subsequent investigation of migraine patients with side-fixed visual aura. We applied a method for comparing cerebral hemispheres from voxelized MRI data by comparison of mirrored data to the original data. In a small sample of 5 neurologically and ophthalmologically healthy subjects, this method showed a clear activation of visual cortex in "stimulated" compared to "non-stimulated" hemispheres. We therefore consider the method valid for the purpose of interhemispheric comparison. The applied stimulus caused activation of a large part of the cerebral cortex, in accordance with the general observation that more than 25 % of the brain is involved in visual processing (58). Thus, the stimulation method allowed us to study not only the early cortical visual areas but also areas of higher-level visual processing. Finally, Study I showed that the

cortical responses to visual stimulation, at least to this particular stimulation, are asymmetrically distributed between the hemispheres. We found some of this lateralization to be dependent on age and increased right hemisphere grey matter volume, but not on handedness, gender, ocular dominance or visual acuity. This finding emphasizes the importance of including a balanced number of patients with left-sided and right-sided symptoms to avoid bias due to physiological left-to-right differences. It further highlights that careful age-matching is necessary for the comparison of two groups, e.g. patients and controls. Therefore in the subsequent studies, 10 patients with left-sided and 10 patients with right-sided visual symptoms were included and control subjects were individually matched for age and gender. In addition, patients with left-sided and right-sided symptoms were of equal age (mean age 34.7 vs. 35.2 years).

The physiological background of the observed left-to-right asymmetry of responsiveness to stimulation in the healthy subject is unknown. A left visual field and corresponding right hemisphere advantage has been reported for several aspects of vision such as face recognition (59), visual change detection (60) and visual attention (61). In a recent study, the threshold for eliciting visual perception was significantly lower in the right hemisphere compared to the left hemisphere when applying direct electrical stimulation to the cortex of awake subjects, suggesting increased neuronal excitability (62). Interestingly, this effect was observed in almost the exact same areas where we observed right hemisphere dominance in the present study.

INCREASED RESPONSIVENESS IN CEREBRAL HEMISPHERES PRODUCING AURA SYMPTOMS (STUDY II)

The major result of study II was that fMRI-BOLD signals to visual stimulation were increased in several non-occipital cortical areas (inferior frontal gyrus, SPL, IPL and IPS) of the symptomatic hemispheres of migraine patients with side-fixed aura. Hyperresponsiveness of these areas was also seen in the symptomatic hemispheres of patients to age and sex matched healthy controls.

The hyperresponsive cortical areas are involved in advanced visual processing (63), especially performance of visuospatial tasks, i.e. localization of objects in space and guidance of actions, eye-movements and shifts of spatial attention (64-67). The frontal regions with hyper-responsiveness further include dorso-lateral prefrontal areas that are engaged in memory-guided saccades and spatial working memory (68,69). The study thus highlights a very specific and lateralized alteration of a cortical network comprising these functions in migraine with unilateral aura.

Accordingly, previous studies have demonstrated that parts of visual function supported by these cortical areas are impaired in MA patients. The patients perform slower on tests of visual attention and visual memory outside of attacks compared to MO patients and healthy controls (70). Deficits of motion perception and orientation discrimination were also found in MA interictally (71). MA patients with side-fixed aura experience visual illusions of motion and orientation in the affected hemifield when viewing stripe patterns (72). MA patients find these patterns more unpleasant than MO patients and controls (73). Dysfunction of saccadic eye movements in migraine has been reported (74,75), although not consistently (76). It is possible that these abnormalities of visual function in migraine patients are correlated to the hyper-responsiveness of the cortical visual areas found in the present study and, thus, that the altered function of this network may explain visual dysfunction in MA. Abnormalities of motion processing in migraine has previously been related to anatomical alterations of cortical areas MT/V5 and V3A (77). In the present study we specifically studied the activation of these areas in the ROI based analysis and found no interhemispheric functional differences. While MT/V5 plays an integral role in motion perception, prefrontal and parietal areas are probably equally important at least for some types of motion perception (78,79).

These findings of hyperresponsivity of higher-level visual cortical areas specifically were surprising, since MA patients theoretically would be expected to show hyperexcitability of the primary visual cortex. In animal models cortex with high neuronal density has the lowest threshold for eliciting CSD, and in humans the cortical area with the highest neuronal density is V1. Based on the current observations, development of migraine aura is not as simple as V1 hyperexcitability causing CSD waves that initiate in V1.

Due to the short-lasting and unpredictable nature of migraine aura, very few neuroimaging studies have investigated the aura phase. These investigations have challenged the notion of V1 as the origin of CSD during visual aura. In the seminal studies of regional cerebral blood flow (rCBF) by Olesen et al. and Lauritzen et al., flow changes of frontal and parietal cortical areas were seen in some cases prior to occipital involvement during visual aura (13,80). More recently a study applying fMRI and visual stimulation recorded a spreading decrease of the BOLD signal starting in visual area V3a at the onset of visual aura (15). It is thus possible that CSD during aura is initiated in higher-level visual cortex. However, involvement of V1 in visual migraine aura should not be ruled out. Another possible explanation is that hyperexcitable higher-level cortical areas may provide the trigger for a CSD wave in V1. There is evidence that higher-level visual areas project back to V1 (81) but this has previously not been related to setting the threshold for spreading depression. It should also be noted that since the BOLD response primarily reflects input and local processing of neuronal information rather than the output (29) it is theoretically possible that the observed increased activity reflect hyperresponsiveness of structures that provide efferent input to these areas.

In a recent study, applying a method very similar to that of Study II, Datta et al. also reported increased BOLD signals in MA patients compared to patients with migraine without aura and to healthy controls (82), but these were located in V1 and LGN. The stimulation used by Datta et al. was designed to maximize V1 responses, while we here used a larger stimulus designed to activate V1 and large expanses of extra-striate cortex. It is possible that the differences in the visual stimulation paradigms account for this discrepancy.

The findings of the present study suggest that MA patients with alternating aura sides or bilateral auras would have no or little interhemispheric differences while still being hyperresponsive compared to healthy controls. This should however be confirmed in future studies and at present our conclusions directly apply to patients with side-fixed aura only.

NO GREY MATTER STRUCTURAL DIFFERENCES RELATED TO LATERALIZED AURA (STUDY III)

In study III we found that side fixed aura is not associated with intherhemispheric grey matter asymmetry in MA patients. A post-hoc analysis comparing the typical migraine headache side of the patients to the contralateral side showed a difference in cortical thickness of the inferior frontal gyrus but no differences detectable by VBM.

Previous studies using only VBM have compared structural MRI data of mixed groups of migraine patients with and without aura to healthy controls (83-88). Results are conflicting, but overall suggest decreases in grey matter density in frontal and cingulate

cortex of migraine patients. To our knowledge, there are no reports of VBM abnormalities in MA specifically. Increased cortical thickness in the visual areas V3a and MT+ has been reported in MA patients compared to healthy controls, but not compared to patients with migraine without aura (77). A study by the same group reported thickening of the somatosensory cortex in a mixed group of migraine patients (with and without aura) compared to controls (89). Datta et al. found no differences in cortical thickness between groups in a large sample of migraine patients with and without aura and matched controls (90).

The results of study III suggest that if structural cerebral grey matter abnormalities occur in migraine patients, these abnormalities are not related to the presence of aura. I.e. cortical dysfunction in MA patients causing aura symptoms is not reflected in structural cortical changes.

Since no VBM or SBM differences were found in the primary analysis comparing symptomatic to asymptomatic hemispheres, we did not compare the hemispheres of patients to hemispheres of controls. As suggested by the previous studies, structural abnormalities may be found on a whole-brain level in migraine patients. Investigating this study question was not within the scope of study III. This would ideally require comparison of large samples of patients with and without aura as well as matched healthy controls.

In study III we additionally found a difference in cortical thickness of the inferior frontal gyrus related to migraine pain (in patients with unilateral headache, N=13). The magnitude of this interhemispheric difference was positively correlated with the attack frequency. The inferior frontal gyrus is part of the central pain processing network (91) and probably contributes to pain modulation/inhibition (92). The observed asymmetry could therefore indicate structural reorganization of pain inhibitory circuits in response to the repeated intense nociceptive input due to the headache attacks.

METHODOLOGICAL CONSIDERATIONS

For the interhemispheric comparison of left vs. right hemispheres in healthy subjects we sought to reduce factors that could produce left-to-right asymmetry bias. We ensured the symmetry of the stimulus by flipping the video goggles and we took into account several lateralized physiological parameters (handedness, visual acuity, and ocular dominance). Asymmetry caused by the MRI acquisition cannot be entirely ruled out. In the MRI acquisition phase encoding of the echo planar imaging sequence was carried out in the anterior-posterior direction to avoid left-right bias. Since the BOLD responses were "baseline corrected" by subtracting signals during rest periods from signals during stimulation periods, magnetic field inhomogeneities would not be expected to influence the results, since these would not affect the magnitude of the relative signal increase. Theoretically, the scanner could also cause stimulus asymmetry by distorting image quality in the video goggles, but this effect seems unlikely. Thus, we believe that the interhemispheric differences reported here represent true physiological effects and not artifacts due to technical issues.

Regardless of these issues, left-to-right bias would not be expected to affect the results of Studies II and III since and equal number of right and left symptomatic hemispheres were studied. Since the two studies in patients were cross-sectional it was not possible to determine whether the observed findings were causes or consequences of the disorder. Aura side was not determined prospectively but simply by asking the patients. Patients could have reported the wrong side. To avoid this type of error only patients with frequent attacks who reported occurrence on the same side in 90% of attacks or more were included. For the headache side patients were only asked which side was their typical headache side and no threshold was applied, meaning that the reported headache side is more error prone. The relation of grey matter structure to headache side was only studied in a subset of patients with unilateral headache. A limitation of this analysis was that it did not include an equal number of left and right hemispheres (8 right, 5 left). The difference could therefore theoretically reflect left-right asymmetry.

CONCLUSIONS

Based on the three studies, we conclude the following:

- The proposed method of "brain flipping" is useful for interhemispheric comparison of fMRI data
- The visual stimulus used in the studies activates large expanses of cortical areas. It is thus not restricted to specially functioning visual areas, rather it appears useful for general assessment of cortical areas involved in visual processing
- In neurologically healthy subjects, the cortical responses to full-field symmetrical stimulation is asymmetrically distributed between the cerebral hemispheres
- Symptomatic hemispheres in migraine patients with unilateral visual aura show an increased BOLD signal in several visually driven areas compared to the contralateral, asymptomatic hemispheres
- Compared to corresponding hemispheres of matched healthy controls, symptomatic hemispheres show larger BOLD responses in the same cortical areas
- No areas of asymptomatic hemispheres in these patients show larger BOLD responses of compared to the contralateral, symptomatic hemispheres
- Compared to corresponding hemispheres of matched healthy controls, asymptomatic are not different in BOLD responses to visual stimulation
- No differences in grey matter structure was observed using a highly sensitive analysis design and two complimentary methods comparing symptomatic with asymptomatic hemispheres in the patients
- An exploratory analysis, comparing the typical migraine headache side of the patients to the contralateral side revealed a difference in cortical thickness in the inferior frontal gyrus but no differences in grey matter density.

Collectively, the findings suggest a hyperexcitability of the visual system in the interictal phase of migraine with visual aura. In addition, they may explain previous findings of visual dysfunction in migraine with aura and they emphasize the importance of cortex outside of the primary visual area. We found no abnormalities of cortical or subcortical grey matter structure related to aura. In contrast, a difference in cortical thickness related to migraine headache lateralization was found in a frontal brain area potentially contributing to pain inhibition.

CONCLUDING REMARKS AND FUTURE PERSPECTIVES

The investigations presented in this thesis provide new insights into the understanding of migraine with aura, especially the observation that visual cortical areas of the brain respond greater in hemispheres that produce aura compared to non aura-producing hemispheres. Based on these findings patients with migraine aura can be informed that they have a hyperresponsive brain but no aura-related structural cortical abnormalities. However, the con-

clusions of the present studies in principle only generalize to patients with side-fixed aura specifically. The findings could therefore benefit from confirmation from studies comparing patients with alternating aura sides to healthy controls, which, due to the difference in study design, would likely require much larger patient sample sizes. Since the observation of increased cortical thickness contralateral to the headache side was based on an exploratory analysis this is in need of confirmation from future studies. Such future confirmatory MRI studies would especially be interesting if performed using ultra-high field (7 tesla) scanners, which allow for much improved spatial resolution. At present, no biomarker of migraine exists. If confirmed, these findings could therefore facilitate the diagnosis and monitoring of migraine with aura. As these studies were cross-sectional, it could not be concluded if the observed hyperresponsiveness was a cause or a consequence of aura. It is indeed possible that attacks of migraine with aura, i.e. repeated waves of CSD, could cause increased cortical excitability (93). This could be resolved by longitudinal studies of newly diagnosed patients that are subsequently scanned after having experienced multiple attacks. The validated method for direct interhemispheric comparison of fMRI data could prove useful for a wide range of different future studies of asymmetry of cerebral function in health and disease.

The increased BOLD responses observed in these studies possibly reflect increased neuronal excitability, but could indicate abnormalities of neurovascular coupling or pial arteriolar reactivity. Stimulation of these areas by TMS or transcranial direct current stimulation could potentially clarify what cortical functions are involved and determine if the cortex is hyperexcitable. If these cortical regions prove to be important for migraine aura generation, it would further be interesting to study the areas at the cellular level. Identification of characteristic profiles of neurotransmitter receptors or ion channels could be useful for development of future pharmacological treatment. Transcranial stimulation could even have the potential to trigger aura, providing the possibility of an experimental human model of aura. Such a model could be highly beneficial to future studies of migraine with aura, e.g. to further clarify what mechanisms are involved in aura initiation and to provide definite evidence of CSD as the underlying cause of aura. This could also clarify the important question whether aura triggers the headache phase or if aura is an epiphenomenon, i.e. that aura is initiated by the event that triggers the headache phase. In conclusion, the present studies contribute to our knowledge of migraine aura pathophysiology of the cerebral cortex but also give rise to new questions. Migraine aura remains one of the most intriguing aspects of the headache disorders. Future studies are needed to further unravel the mechanisms of this phenomenon to the benefit of migraine sufferers.

LIST OF ABBREVIATIONS

BOLD blood-oxygenation level dependent
CBF cerebral blood flow
CSD cortical spreading depression
fMRI functional magnetic resonance imaging
FOV field of view
MA migraine with aura
MNI Montreal Neurological Institute
MO migraine without aura
MRI magnetic resonance imaging
TMS transcranial magnetic stimulation
VBM voxel-based morphometry
VEP visual evoked potential

SUMMARY

Migraine sufferers with aura often report visual discomfort outside of attacks and many consider bright or flickering light an attack-precipitating factor. The nature of this visual hypersensitivity and its relation to the underlying pathophysiology of the migraine aura is unknown. A useful technology to study these features of migraine with aura (MA) is functional magnetic resonance imaging (fMRI), which has the potential not only to detect, but also to localize hypersensitive cortex. The main objective of this thesis was to investigate the cortical responsivity of patients with MA during visual stimulation using fMRI. To optimize sensitivity, we applied a within-patient design by assessing functional interhemispheric differences in patients consistently experiencing visual aura in the same visual hemifield.

To validate our data analysis methods, we initially studied healthy volunteers using single hemi-field visual stimulation and compared the “stimulated” hemispheres (i.e. hemispheres contralateral to the visual stimulation) to the “non-stimulated” hemispheres. We then applied this validated method of interhemispheric comparison of fMRI-blood oxygenation level dependent (BOLD) activation to compare left versus right hemisphere responses to symmetric full-field visual stimulation in 54 healthy subjects (study I).

This study concluded that, a) the applied visual stimulation is effective in activating large expanses of visual cortex, b) interhemispheric differences in fMRI-BOLD activation can be determined using the proposed method, and c) visual responses to symmetric full-field visual stimulation are asymmetrically distributed between the cerebral hemispheres. We investigated the effects of migraine aura, by including 20 patients with frequent side-fixed visual aura attacks, i.e. >= 90% of auras occurring in the same visual hemifield (study II). To circumvent bias relating to differences between right and left hemispheres (e.g. caused by physiological left/right bias, asymmetry of the visual stimulation or magnetic field inhomogeneity of the scanner), we included an equal number of patients with right- and left-sided symptoms. Further, we included 20 individually matched healthy controls with no history (including family history) of migraine. We compared the fMRI-BOLD responses to visual stimulation between symptomatic and asymptomatic hemispheres during the interictal phase and between migraine patients and controls. BOLD responses were selectively increased in the in the symptomatic hemispheres and localized in the inferior parietal lobule, the inferior frontal gyrus and the superior parietal lobule. The affected cortical areas comprise a visually driven functional network involved in oculomotor control, guidance of movement, motion perception, visual attention, and visual spatial memory. The patients also had significantly increased response in the same cortical areas when compared to controls.

Since these findings theoretically could depend on aura-related differences in brain structure, we performed additional analyses (study III) to determine the relation between migraine aura and structural, cortical and subcortical, grey matter abnormalities. We analyzed structural MRI data from the same 20 patients and applied voxel-based morphometry and surface-based morphometry on a whole-hemisphere level and for specific anatomical regions of interest. Within-subject comparisons were made with regard to aura symptoms (N=20 vs 20) and with regard to headache (N=13 vs 13). We found no differences in grey matter structure with regard to aura symptoms in MA patients. Comparing the typical migraine headache side of the patients to the contralateral side revealed a difference in cortical thickness in the inferior

frontal gyrus, which correlated significantly with the migraine attack frequency.

In conclusion, we validated a method of interhemispheric comparison of fMRI-BOLD responses to visual stimulation. By using this method we discovered a lateralized alteration of a visually driven functional network in patients with side-fixed aura. These findings suggest a hyperexcitability of the visual system in the interictal phase of migraine with visual aura. Further, this abnormal function is not dependent on lateralized abnormalities of gray matter structure. However, alteration of the inferior frontal cortex related to headache lateralization could indicate structural reorganization of pain inhibitory circuits in response to the repeated intense nociceptive input due to the headache attacks.

REFERENCES

1. Hougaard A, Jensen BH, Amin FM, Rostrup E, Hoffmann MB, Ashina M. Cerebral Asymmetry of fMRI-BOLD Responses to Visual Stimulation. PLoS ONE. 2015 May 18;10(5).
2. Hougaard A, Amin FM, Hoffmann MB, Rostrup E, Larsson HBW, Asghar MS, et al. Interhemispheric differences of fMRI responses to visual stimuli in patients with side-fixed migraine aura. Hum Brain Mapp. 2014 Jun;35(6):2714–23.
3. Hougaard A, Amin FM, Hoffmann MB, Larsson HBW, Magon S, Sprenger T, et al. Structural gray matter abnormalities in migraine relate to headache lateralization, but not aura. Cephalalgia. 2015 Jan;35(1):3–9.
4. Stovner LJ, Hagen K, Jensen R, Katsarava Z, Lipton RB, Scher AI, et al. The global burden of headache: a documentation of headache prevalence and disability worldwide. Cephalalgia. 2007 Mar;27(3):193–210.
5. Hawkins K, Wang S, Rupnow M. Direct cost burden among insured US employees with migraine. Headache. 2008 Apr;48(4):553–63.
6. Hawkins K, Wang S, Rupnow MFT. Indirect cost burden of migraine in the United States. J Occup Environ Med. 2007 Apr;49(4):368–74.
7. Sobocki PA, Jönsson B, Wittchen H-UW, Olesen J. Cost of disorders of the brain in Europe. Eur J Neurol. 2005 Jun;12(Suppl.):1–27.
8. Tfelt-Hansen P, Olesen J. Taking the negative view of current migraine treatments: the unmet needs. CNS Drugs. 2012 May 1;26(5):375–82.
9. Headache Classification Committee of the International Headache Society (IHS). The International Classification of Headache Disorders, 3rd edition (beta version). Cephalalgia. 2013 Jul;33(9):629–808.
10. Russell M, Olesen J. A nosographic analysis of the migraine aura in a general population. Brain. 1996;119:355–61.
11. Lashley KS. Patterns of cerebral integration indicated by the scotomas of migraine. Arch NeurPsych. 1941;46(2):331-339
12. Leao AAP. Spreading depression of activity in the cerebral cortex. J Neurophysiol. American Physiological Society; 1944;7:359–90.
13. Olesen J, Larsen B, Lauritzen M. Focal hyperemia followed by spreading oligemia and impaired activation of rCBF in classic migraine. Ann Neurol. 1981;9(4):344–52.
14. Lauritzen M, Olesen J. Regional cerebral blood flow during migraine attacks by Xenon-133 inhalation and emission tomography. Brain. 1984 Jun;107(2):447–61.
15. Hadjikhani N, Sanchez del Rio M, Wu O, Schwartz D, Bakker D, Fischl B, et al. Mechanisms of migraine aura revealed by functional MRI in human visual cortex. Proceedings of the National Academy of Sciences of the United States of America. 2001;98(8):4687.
16. Dohmen C, Sakowitz OW, Fabricius M, Bosche B, Reithmeier T, Ernestus R-I, et al. Spreading depolarizations occur in human ischemic stroke with high incidence. Ann Neurol. 2008 Jun;63(6):720–8.
17. Strong AJ, Fabricius M, Boutelle MG, Hibbins SJ, Hopwood SE, Jones R, et al. Spreading and Synchronous Depressions of Cortical Activity in Acutely Injured Human Brain. Stroke. 2002 Nov 7;33(12):2738–43.
18. Bolay H, Reuter U, Dunn AK, Huang Z, Boas DA, Moskowitz MA. Intrinsic brain activity triggers trigeminal meningeal afferents in a migraine model. Nat Med. 2002 Feb 1;8(2):136–42.
19. Kelman L. The triggers or precipitants of the acute migraine attack. Cephalalgia. 2007 May 1;27(5):394–402.
20. Hauge AW, Kirchmann M, Olesen J. Trigger factors in migraine with aura. Cephalalgia. 2010 Mar 1;30(3):346–53.
21. Russell M, Rasmussen B, Fenger K, Olesen J. Migraine without aura and migraine with aura are distinct clinical entities: a study of four hundred and eighty-four male and female migraineurs from the general population. Cephalalgia. 1996 Jun;16(4):239–45.
22. Main A, Dowson A, Gross M. Photophobia and phonophobia in migraineurs between attacks. Headache. 1997 Sep;37(8):492–5.
23. Drummond PD. A quantitative assessment of photophobia in migraine and tension headache. Headache. 1986 Oct;26(9):465–9.
24. Haigh S, Karanovic O, Wilkinson F, Wilkins A. Cortical hyperexcitability in migraine and aversion to patterns. Cephalalgia. 2012 Feb 13;32(3):236–40.
25. Brigo F, Storti M, Nardone R, Fiaschi A, Bongiovanni LG, Tezzon F, et al. Transcranial magnetic stimulation of visual cortex in migraine patients: a systematic review with meta-analysis. J Headache Pain. 2012 Jul;13(5):339–49.
26. Welch KM, D'Andrea G, Tepley N, Barkley G, Ramadan NM. The concept of migraine as a state of central neuronal hyperexcitability. Neurologic Clinics of NA. 1990 Nov;8(4):817–28.
27. Aurora SK, Wilkinson F. The brain is hyperexcitable in migraine. Cephalalgia. 2007 Dec;27(12):1442–53.
28. van Harreveld A, Stamm JS. Cortical responses to metrazol and sensory stimulation in the rabbit. Electroencephalography and Clinical Neurophysiology. 1955 Aug;7(3):363–70.
29. Logothetis NK, Wandell BA. Interpreting the BOLD signal. Annu Rev Physiol. 2004;66:735–69.
30. Huang J, Zong X, Wilkins A, Jenkins B, Bozoki A, Cao Y. fMRI evidence that precision ophthalmic tints reduce cortical hyperactivation in migraine. Cephalalgia. 2011 Jun;31(8):925-36
31. Huang J, Cooper TG, Satana B, Kaufman DI, Cao Y. Visual distortion provoked by a stimulus in migraine associated with hyperneuronal activity. Headache. 2003 Jun;43(6):664–71.

32. Vincent M, Pedra E, Mourão-Miranda J, Bramati IE, Henrique AR, Moll J. Enhanced interictal responsiveness of the migraineous visual cortex to incongruent bar stimulation: a functional MRI visual activation study. Cephalalgia. 2003 Nov;23(9):860–8.
33. Watkins KE, Paus T, Lerch JP, Zijdenbos A, Collins DL, Neelin P, et al. Structural asymmetries in the human brain: a voxel-based statistical analysis of 142 MRI scans. Cereb Cortex. 2001 Sep;11(9):868–77.
34. Good CD, Johnsrude I, Ashburner J, Henson RNA, Friston KJ, Frackowiak RSJ. Cerebral Asymmetry and the Effects of Sex and Handedness on Brain Structure: A Voxel-Based Morphometric Analysis of 465 Normal Adult Human Brains. Neuroimage. 2001 Sep;14(3):685–700.
35. Baciu M, Juphard A, Cousin E, Bas JFL. Evaluating fMRI methods for assessing hemispheric language dominance in healthy subjects. Eur J Radiol. 2005 Aug;55(2):209–18.
36. The International Classification Of Headache Disorders, 2nd edition. Cephalalgia. 1st ed. 2004 Jan 1;24:1–160.
37. Oldfield RC. The assessment and analysis of handedness: the Edinburgh inventory. Neuropsychologia. 1971 Mar;9(1):97–113.
38. Bach M. The Freiburg Visual Acuity Test-Variability unchanged by post-hoc re-analysis. Graefes Arch Clin Exp Ophthalmol. 2007 Jan 12;245(7):965–71.
39. Miles WR. Ocular dominance in human adults. J Gen Psychol. 1930; 3(3):412-30.
40. Wolynski B, Schott BH, Kanowski M, Hoffmann MB. Visuo-motor integration in humans: Cortical patterns of response lateralisation and functional connectivity. Neuropsychologia. 2009 Apr;47(5):1313–22.
41. Jenkinson M, Beckmann CF, Behrens TEJ, Woolrich MW, Smith SM. FSL. Neuroimage. 2012 Aug 15;62(2):782–90.
42. Oakes TR, Fox AS, Johnstone T, Chung MK, Kalin N. Integrating VBM into the general linear model with voxelwise anatomical covariates. Neuroimage. 2007 Jan 15;34(2):500-8.
43. Eickhoff SB, Heim S, Zilles K, Amunts K. Testing anatomically specified hypotheses in functional imaging using cytoarchitectonic maps. Neuroimage. 2006 Aug 15;32(2):570–82.
44. Holm S. A simple sequentially rejective multiple test procedure. Scandinavian journal of statistics. JSTOR; 1979;:65–70.
45. Dale AM, Fischl B, Sereno MI. Cortical surface-based analysis. I. Segmentation and surface reconstruction. Neuroimage. 1999 Feb;9(2):179–94.
46. Fischl B, Dale AM. Measuring the thickness of the human cerebral cortex from magnetic resonance images. PNAS. 2000 Sep 26;97(20):11050–5.
47. Hinds OP, Rajendran N, Polimeni JR, Augustinack JC, Wiggins G, Wald LL, et al. Accurate prediction of V1 location from cortical folds in a surface coordinate system. Neuroimage. 2008 Feb 15;39(4):1585–99.
48. Benson NC, Butt OH, Datta R, Brainard DH, Aguirre GK. A Universal Retinotopic Mapping of V1 with Respect to Anatomy. J Vision. 2011 Sep 23;11(11):1067–7.
49. Hutton C, Draganski B, Ashburner J, Weiskopf N. A comparison between voxel-based cortical thickness and voxel-based morphometry in normal aging. Neuroimage. 2009 Nov 1;48(2):371–80.
50. Douaud G, Smith S, Jenkinson M, Behrens T, Johansen-Berg H, Vickers J, et al. Anatomically related grey and white matter abnormalities in adolescent-onset schizophrenia. Brain. 2007 Sep;130(Pt 9):2375–86.
51. Good CD, Johnsrude IS, Ashburner J, Henson RN, Friston KJ, Frackowiak RS. A voxel-based morphometric study of ageing in 465 normal adult human brains. Neuroimage. 2001 Jul;14(1 Pt 1):21–36.
52. Smith SM, Jenkinson M, Woolrich MW, Beckmann CF, Behrens TEJ, Johansen-Berg H, et al. Advances in functional and structural MR image analysis and implementation as FSL. Neuroimage. 2004;23 Suppl 1:S208–19.
53. Andersson J, Jenkinson M, Smith S. Non-linear registration, aka Spatial normalisation. FMRIB technical report TR07JA2. 2007.
54. Nichols TE, Holmes AP. Nonparametric permutation tests for functional neuroimaging: a primer with examples. Hum Brain Mapp. 2002 Jan;15(1):1–25.
55. Smith SM, Nichols TE. Threshold-free cluster enhancement: addressing problems of smoothing, threshold dependence and localisation in cluster inference. Neuroimage. 2009 Jan 1;44(1):83–98.
56. Greve DN, Van der Haegen L, Cai Q, Stufflebeam S, Sabuncu MR, Fischl B, et al. A surface-based analysis of language lateralization and cortical asymmetry. J Cogn Neurosci. 2013 Sep;25(9):1477–92.
57. Fischl B, Sereno MI, Tootell RB, Dale AM. High-resolution intersubject averaging and a coordinate system for the cortical surface. Hum Brain Mapp. 1999;8(4):272–84.
58. Baker CI. Visual Processing in the Primate Brain. In: Weiner IB, editor. Handbook of Psychology. 2nd ed. Hoboken, NJ: John Wiley & Sons; 2012. pp. 81–114.
59. Yovel G, Tambini A, Brandman T. The asymmetry of the fusiform face area is a stable individual characteristic that underlies the left-visual-field superiority for faces. Neuropsychologia. 2008 Nov;46(13):3061–8.
60. Verleger R, Sprenger A, Gebauer S, Fritzmannova M, Friedrich M, Kraft S, et al. On why left events are the right ones: neural mechanisms underlying the left-hemifield advantage in rapid serial visual presentation. J Cogn Neurosci. 2009 Mar;21(3):474–88.
61. Thiebaut de Schotten M, Dell'Acqua F, Forkel SJ, Simmons A, Vergani F, Murphy DGM, et al. A lateralized brain network for visuospatial attention. Nat Neurosci. 2011 Oct;14(10):1245–6.
62. Jonas J, Frismand S, Vignal J-P, Colnat-Coulbois S, Koessler L, Vespignani H, et al. Right hemispheric dominance of visual phenomena evoked by intracerebral stimulation of the human visual cortex. Hum Brain Mapp. 2014 Jul;35(7):3360-71.
63. Van Essen DC, Gallant JL. Neural mechanisms of form and motion processing in the primate visual system. Neuron. 1994 Jul;13(1):1–10.
64. Rizzolatti G, Matelli M. Two different streams form the dorsal visual system: anatomy and functions. Exp Brain Res. 2003 Nov 1;153(2):146–57.
65. Swisher JD, Halko MA, Merabet LB, McMains SA, Somers DC. Visual Topography of Human Intraparietal Sulcus. J Neurosci. 2007 May 16;27(20):5326–37.
66. Perani D, Vallar G, Cappa S, Messa C, Fazio F. Aphasia and neglect after subcortical stroke. A clinical/cerebral

perfusion correlation study. Brain. 1987 Oct;110 (Pt 5):1211–29.
67. Rizzolatti G, Matelli M. Two different streams form the dorsal visual system: anatomy and functions. Exp Brain Res. 2003 Nov 1;153(2):146–57.
68. Walker R, Husain M, Hodgson TL, Harrison J. Saccadic eye movement and working memory deficits following damage to human prefrontal cortex. Neuropsychologia. 1998 Nov;36(11):1141-59.
69. Seeck M, Schomer D, Mainwaring N, Ives J, Dubuisson D, Blume H, et al. Selectively distributed processing of visual object recognition in the temporal and frontal lobes of the human brain. Ann Neurol. 1995 Apr;37(4):538–45.
70. Mulder E, Linssen W, Passchier J, Orlebeke JF, Geus EJC. Interictal and postictal cognitive changes in migraine. Cephalalgia. 2009;19(6):557–65.
71. McKendrick AM, Vingrys AJ, Badcock DR, Heywood JT. Visual dysfunction between migraine events. Invest Ophthalmol Vis Sci. 2001 Mar;42(3):626–33.
72. Khalil NM, Nicotra A, Wilkins AJ. Asymmetry of visual function in migraine with aura: Correlation with lateralisation of headache and aura. Cephalalgia. 2011 Jan 20;31(2):213–21.
73. Chronicle EP, Wilkins AJ, Coleston DM. Thresholds for detection of a target against a background grating suggest visual dysfunction in migraine with aura but not migraine without aura. Cephalalgia. 1995;15(2):117–22.
74. Cambron M, Anseeuw S, Paemeleire K, Crevits L. Saccade behaviour in migraine patients. Cephalalgia. 2011 Jul 15;31(9):1005–14.
75. Chandna A, Chandrasekharan DP, Ramesh AV, Carpenter R. Altered interictal saccadic reaction time in migraine: a cross-sectional study. Cephalalgia. 2012 May 31;32(6):473–80.
76. Wilkinson F, Karanovic O, Ross EC, Lillakas L, Steinbach MJ. Ocular motor measures in migraine with and without aura. Cephalalgia. 2006 Jun;26(6):660–71.
77. Granziera C, DaSilva AFM, Snyder J, Tuch DS, Hadjikhani N. Anatomical Alterations of the Visual Motion Processing Network in Migraine with and without Aura. PLoS Med. 2006;3(10):e402.
78. Billino J, Braun DI, Böhm K-D, Bremmer F, Gegenfurtner KR. Cortical networks for motion processing: Effects of focal brain lesions on perception of different motion types. Neuropsychologia. 2009 Aug;47(10):2133–44.
79. Bremmer F, Schlack A, Shah NJ, Zafiris O, Kubischik M, Hoffmann K, et al. Polymodal motion processing in posterior parietal and premotor cortex: a human fMRI study strongly implies equivalencies between humans and monkeys. Neuron. 2001 Jan;29(1):287–96.
80. Lauritzen M, Olesen J. Regional cerebral blood flow during migraine attacks by Xenon-133 inhalation and emission tomography. Brain. 1984 Jun;107 (Pt 2):447–61.
81. Lauritzen TZ, D'Esposito M, Heeger DJ, Silver MA. Top-down flow of visual spatial attention signals from parietal to occipital cortex. J Vision. 2009 Dec 1;9(13):18–8.
82. Datta R, Aguirre GK, Hu S, Detre JA, Cucchiara B. Interictal cortical hyperresponsiveness in migraine is directly related to the presence of aura. Cephalalgia. 2013 Apr;33(6):365-74.
83. Schmidt-Wilcke T, Gänßbauer S, Neuner T, Bogdahn U, May A. Subtle grey matter changes between migraine patients and healthy controls. Cephalalgia. 2008 Jan;28(1):1-4.
84. Rocca MA. Brain Gray Matter Changes in Migraine Patients With T2-Visible Lesions: A 3-T MRI Study. Stroke. 2006 May 25;37(7):1765–70.
85. Jin C, Yuan K, Zhao L, Zhao L, Yu D, Deneen von KM, et al. Structural and functional abnormalities in migraine patients without aura. NMR Biomed. 2012 Jun 7;26(1):58–64.
86. Valfrè W, Rainero I, Bergui M, Pinessi L. Voxel-Based Morphometry Reveals Gray Matter Abnormalities in Migraine. Headache. 2007 Dec 20;48(1):109–17.
87. Kim J, Suh S-I, Seol H, Oh K, Seo W-K, Yu S-W, et al. Regional grey matter changes in patients with migraine: a voxel-based morphometry study. Cephalalgia. 2008 Jun;28(6):598–604.
88. Matharu MS, Good CD, May A, Bahra A, Goadsby PJ. No change in the structure of the brain in migraine: a voxel-based morphometric study. Eur J Neurol. 2003 Jan;10(1):53–7.
89. DaSilva AFM, Granziera C, Snyder J, Hadjikhani N. Thickening in the somatosensory cortex of patients with migraine. Neurology. 2007 Nov 20;69(21):1990–5.
90. Datta R, Detre JA, Aguirre GK, Cucchiara B. Absence of changes in cortical thickness in patients with migraine. Cephalalgia. 2011 Oct;31(14):1452-8.
91. Tracey I. Imaging pain. Br J Anaesth. 2008 Apr 19;101(1):32–9.
92. Lorenz J, Cross DJ, Minoshima S, Morrow TJ, Paulson PE, Casey KL. A unique representation of heat allodynia in the human brain. Neuron. 2002 Jul 18;35(2):383–93.
93. Berger M, Speckmann E-J, Pape HC, Gorji A. Spreading depression enhances human neocortical excitability in vitro. Cephalalgia. 2008 May;28(5):558–62.